Inorganic Chemistry

Article

pubs.acs.org/IC

NHC Copper(I) Complexes Bearing Dipyridylamine Ligands: Synthesis, Structural, and Photoluminescent Studies

Ronan Marion,[†] Fabien Sguerra,[‡] Florent Di Meo,[§] Elodie Sauvageot,[†] Jean-François Lohier,[†] Richard Daniellou,[⊥] Jean-Luc Renaud,[†] Mathieu Linares,*[,§] Matthieu Hamel,*[,‡] and Sylvain Gaillard*[,†]

[†]Laboratoire de Chimie Moléculaire et Thioorganique, Normandie University, Université de Caen Basse Normandie, CNRS, UMR 6507, 6, Boulevard du Maréchal Juin, 14050 Caen, France

[‡]Laboratoire Capteurs et Architectures Electroniques, CEA, LIST, F-91191 Gif-sur-Yvette Cedex, France

[§]Department of Physics, Chemistry, and Biology, Linköping University, SE-581 83 Linköping, Sweden

[⊥]Institut de Chimie Organique et Analytique, University of Orléans, CNRS, UMR 7311 45067 Orléans, France

Supporting Information

ABSTRACT: We describe the synthesis of new cationic tricoordinated copper complexes bearing bidentate pyridine-type ligands and N-heterocyclic carbene as ancillary ligands. These cationic copper complexes were fully characterized by NMR, electrochemistry, X-ray analysis, and photophysical studies in different environments. Density functional theory calculations were also undertaken to rationalize the assignment of the electronic structure and the photophysical properties. These tricoordinated cationic copper complexes possess a stabilizing CH−π interaction leading to high stability in both solid and liquid states. In addition, these copper complexes, bearing dipyridylamine ligands having a central nitrogen atom as potential anchoring point, exhibit very interesting luminescent properties that render them potential candidates for organic light-emitting diode applications.

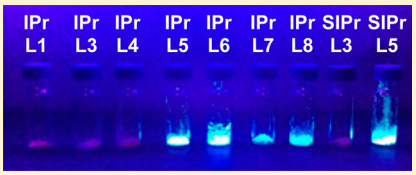

INTRODUCTION

Luminescent material containing heavy metal cores have been extensively studied.[1] For several years, those materials have found many applications in the field of organic light-emitting diode (OLED).[2] Among the transition metals used for this application, iridium, ruthenium, platinum, and gold have been the most extensively described.[2] However, owing to their limited availability, their toxicity and their prices, the substitution of these noble metals by more available ones is of great interest. In this purpose, copper(I) complexes appear to be a good alternative.[3]

In a general manner, organometallic complexes need to possess particular properties for OLED application. Considering molecules dedicated as blue triplet emitters in OLEDs materials, the compounds must exhibit emission around 450 to 470 nm, short phosphorescence lifetime at 298 K, phosphorescence quantum yield at least superior to 0.25 at 298 K, and should ideally be stable toward oxygen and present reversible redox behavior.[4] In this purpose, several architectures, such as tricoordinated,[5] homoleptic polynuclear,[6] and heteroleptic mononuclear[6d,7] copper complexes have been prepared and their photophysical properties have been studied.

Until now, the homoleptic mononuclear copper complex structure did not appear to be promising as only one example was described.[5] Most represented are homoleptic polynuclear copper complexes.[6] Indeed, to overcome the potential flattening distortion of tetrahedral copper complexes in the excited states,[8] the bridged halide atoms led to copper complexes with a blocked geometry.[6a]

Nevertheless, from a conceptual point of view, heteroleptic mononuclear copper complexes seemed also interesting as they allow a broader range of ligand combinations and a finer tuning of the properties. However, the ligand combination is crucial and has to give a structurally rigid copper complex and sterically demanding ligands are usually selected. But, the formation of homoleptic complexes is then a competitive issue. Indeed, dissociation and recombination of ligands can occur and yield to an equilibrium in solution with the formation of both expected heteroleptic and unwanted homoleptic complexes.[9] A perusal of the literature for luminescent heteroleptic copper complexes shows that tetracoordinated copper complexes are often studied and the most represented ligand combination was an association of N^N ligands and diphosphine.[7−10]

N-Heterocyclic carbene (NHC) ligands are now considered as very good candidates for the stabilization of organometallic species[11] and some groups have turned their attention to complexes bearing these ancillary ligands.[12] Such heteroleptic NHC copper(I) complexes possessing luminescent properties are tricoordinated species with the two remaining coordination sites occupied either by a nitrogen-based ligand (phenanthroline or pyridyl azolate)[12b,c] or a diphosphine ligand.[12d]

For several years, one of our research interest has been focused on the synthesis[13] and the coordination[14] of dipyridylamine derivatives because these compounds can be easily functionalized and finely tuned. Moreover, the central nitrogen

Received: May 26, 2014
Published: August 18, 2014

   dx.doi.org/10.1021/ic501230m | Inorg. Chem. 2014, 53, 9181−9191

atom can serve as anchoring point for a covalent bonding to a host polymer, ensuring a morphological stability against interlayer diffusion and crystallization.[6a,15] Such functionalizations of dipyridylamine ligands have already opened a broad range of applications in supported catalysis,[16] ion detection,[17] or OLEDs.[18]

Here, we report the synthesis of an original combination of dipyridylamine and N^N ligands (Figure 1) with NHC ligands

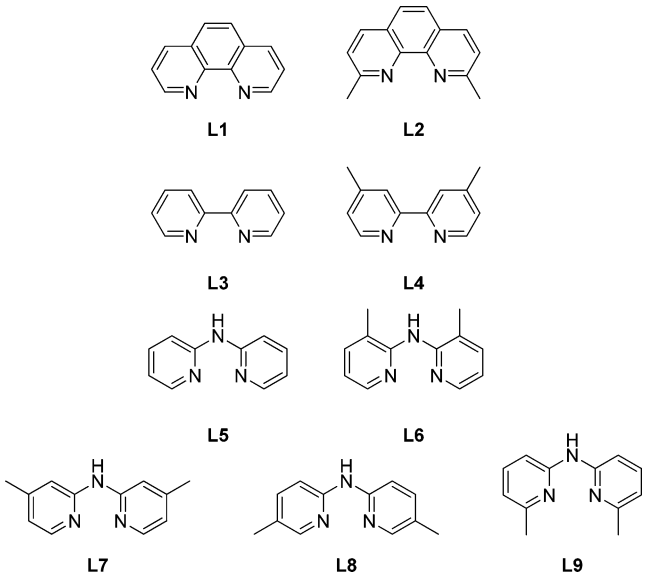

Figure 1. N^N ligands used in this study.

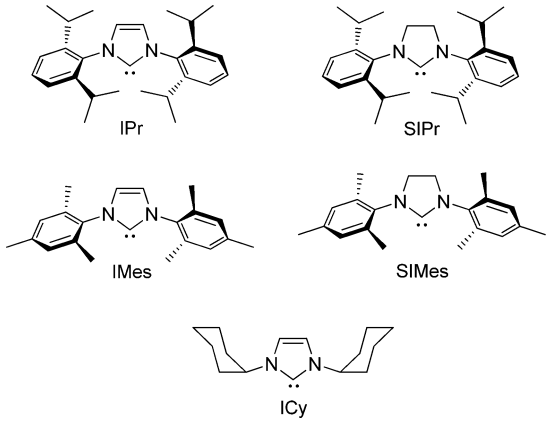

Figure 2. NHC ligands used in this study.

(Figure 2) leading to promising phosphorescent three-coordinate copper(I) complexes of general formula [Cu(NHC)(N^N)][X]. These cationic copper complexes were fully characterized by NMR, electrochemistry, X-ray analysis, and photophysical studies in different environments. Density functional theory (DFT) calculations were also undertaken to rationalize the assignment of the electronic structure and the photophysical properties. In addition, their properties were compared with those of known three-coordinate NHC copper(I) complexes bearing either 2,2′-bipyridine or phenanthroline ligand.[12b] Finally, all these studies pinpoint the important benefit of a CH−π interaction, found in these complexes, which led to a blocked geometry and to highly stable copper(I) complexes exhibiting blue-shift emission.

RESULTS AND DISCUSSION

Complexes Synthesis. This study began with an exploration of the [Cu(NHC)(N^N)][X] synthesis (X = BF_4^- or PF_6^-). All [CuCl(NHC)] precursors were prepared following the Nolan−Cazin procedure using Cu_2O as copper source and imidazolium salts.[19] Dipyridylamines were obtained following our previously described procedure using a Buchwald−Hartwig coupling reaction between 2-bromopyridine and 2-aminopyridine derivatives.[13] Then, addition of the appropriate N^N ligand to a refluxing ethanol solution of [CuCl(NHC)] complex led to the [Cu(NHC)(N^N)][X] complex in good to excellent isolated yields (see Table 1).

Table 1. Synthesis of [Cu(NHC)(N^N)][X] Complexes via [CuCl(NHC)] Precursors[a]

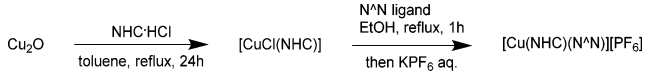

entry	complexes	yield (%)[b]
1	[Cu(IPr)(**L1**)][PF_6] (**1**)	56
2	[Cu(IPr)(**L2**)][PF_6] (**2**)	0
3	[Cu(IPr)(**L3**)][PF_6] (**3**)	72
4	[Cu(IPr)(**L4**)][PF_6] (**4**)	94
5	[Cu(IPr)(**L5**)][PF_6] (**5**)	72
6	[Cu(IPr)(**L6**)][PF_6] (**6**)	98
7	[Cu(IPr)(**L7**)][PF_6] (**7**)	93
8	[Cu(IPr)(**L8**)][PF_6] (**8**)	73
9	[Cu(IPr)(**L9**)][PF_6] (**9**)	0
10	[Cu(SIPr)(**L3**)][PF_6] (**10**)	88
11	[Cu(SIPr)(**L5**)][PF_6] (**11**)	81
12	[Cu(IMes)(**L5**)][PF_6] (**12**)	<5[c]
13	[Cu(SIMes)(**L5**)][PF_6] (**13**)	<5[c]
14	[Cu(ICy)(**L5**)][PF_6] (**14**)	0

[a]Reaction conditions: [CuCl(NHC)] (1 equiv), N^N ligand (1.05 equiv), EtOH, reflux, 1 h. [b]Isolated yield. [c]Signals of the expected complex were observed by ^{1}H NMR analysis, but no complex was isolated from the starting material.

Worth to note, yields depend greatly of the steric hindrance of both ligands as depicted in Table 1. Indeed, when neocuproine (**L2**) or bis(6-methylpyridin-2-yl)amine (**L9**) ligands were mixed with [CuCl(IPr)] (**15**), the expected [Cu(IPr)(N^N)][PF_6] complexes were not observed. Nevertheless, in the case of neocuproine **L2**, both homoleptic [$Cu(IPr)_2$][PF_6][20] and [$Cu(\mathbf{L2})_2$][PF_6][21] complexes were isolated and their structures were confirmed by comparison of the known ^{1}H NMR data and XRD analyses. We assume that the steric hindrance created around the copper center is not compatible with a trigonal planar geometry and led to the disproportionation of the three-coordinate copper complexes into the corresponding homoleptic complexes. This result is also consistent with the observations of Nierengarten during the preparation of heteroleptic copper(I) complexes with sterically hindered phenanthroline derivatives and bis-phosphine ligands.[9] The nature of the *N*-aryl-substituted NHC appeared also to be crucial for the stability of these copper complexes. Indeed, when [CuCl(IMes)] (**16**) was treated in the presence of ligand **L3** or **L5**, less than 5% conversion of the expected complexes was observed by ^{1}H NMR analysis, and

dx.doi.org/10.1021/ic501230m | Inorg. Chem. 2014, 53, 9181−9191

their purifications failed in our hands. In a similar way, when [CuCl(ICy)] (**17**) was introduced with ligand **L5**, no complex was isolated and the starting material was recovered totally unchanged (Table 1, Entry 14).

As alternative to this procedure, the copper hydroxide synthon [CuOH(IPr)] (**18**), reported by Nolan,[22] was also investigated. This procedure was only attempted with non-substituted N^N ligands **L1**, **L3**, and **L5** to demonstrate the proof of concept. Gratifyingly, reactions were carried out in the presence of one equivalent of HBF_4 and provided the desired [Cu(IPr)(N^N)][BF_4] complexes in moderate to good yields (52 to 78%). Results are summarized in Table 2. This

Table 2. Preparation of [Cu(NHC)(N^N)][BF_4] Complexes via [CuOH(IPr)] (18)[a]

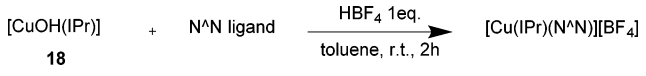

entry	complexes	yield (%)[b]
1	[CuIPr(**L1**)][BF_4] (**19**)	78
2	[CuIPr(**L3**)][BF_4] (**20**)	52
3	[CuIPr(**L5**)][BF_4] (**21**)	78

[a]General conditions: [CuOH(IPr)] (1 equiv), N^N ligand (1 equiv), HBF_4 (1 equiv), toluene, room temperature, 2 h. [b]Isolated yield.

methodology can be an alternative route for the preparation of heteroleptic [Cu(NHC)(N^N)][X] complexes even if the preparation of the [CuOH(IPr)] represents an additional step in this synthesis. Noteworthy, compared to the previously reported method for the synthesis of [Cu(IPr)(**L1**)][OTf] using silver triflate, these two methodologies are silver salts free.[12b]

Then, to evaluate the stability of the [Cu(NHC)(Hdpa)][X] complexes (Hdpa = dipyridylamine derivatives ligands **L5**−**L8**), we decided to stress our complexes in an oven at 90 °C for a week. ^{1}H NMR spectra were recorded and found unchanged, compared with the spectra recorded after isolation of the complex. Then, stability in solution was also investigated, and sample of [Cu(IPr)**L5**][PF_6] (**5**) was prepared in $CDCl_3$.[23] ^{1}H NMR spectra were recorded every day for a week and found unchanged, compared with the spectrum of a freshly prepared copper complex. These control experiments demonstrate clearly the thermal stability of the [Cu(NHC)(Hdpa)][X] and also that no dissociation of ligands occurs in solution.

Crystallographic. To unequivocally determine the atom connectivity in these [Cu(NHC)(N^N)][X] complexes, single crystals for X-ray diffraction (XRD) were grown by slow gas diffusion of pentane into a dichloromethane or chloroform-saturated solution of [Cu(NHC)(N^N)][X] complexes. Figure 3 shows a thermal ellipsoid representation of crystallized complexes [Cu(NHC)(N^N)][X]. Selected bond lengths and angles, as well as the CH···C_g distances are summarized in Table 3 (For crystal data, see Supporting Information, Table S1−S3).

As expected for the dipyridylamine ligands **L5**−**L8**, their coordination to the copper center led to a 6-membered chelate. Interestingly, the hydrogen atoms at the α position related to the nitrogen atom in the pyridine rings interact with the N-substituted phenyl ring of IPr or SIPr ligand. The calculated distances between the centroid of the NHC aromatic ring and the hydrogen atom in α position ranged from 2.43 to 2.97 Å.[24] This interaction may help to stabilize the complex (see the DFT Computational Details). It is worth mentioning that this CH−π interaction in the solid state is also observed in solution by NOESY NMR experiments (Supporting Information, Figure S1).

Then, the N_{ligand}···Cu···N_{ligand} angles in complexes **5**, **6**, **8**, and **11** are equal to 90°(1), 89°(6), 91°(0), and 88°(9), respectively. These values are 10° higher than the angles measured with the five-membered chelates, whatever the N^N ligand (**L1**, **L3**, **L4**). This larger bite angle has a deep effect on the physical properties of these three-coordinate copper complexes (*vide infra*).

Photophysical Study. The absorption and solid emission spectra of copper(I) complexes are given in Table 4 and Figure 4.

The absorption spectra, recorded in $CHCl_3$, show two intense bands. The first one, between 240 and 262 nm (ε = (16−31) × 10^3 L·mol^{-1}·cm^{-1}), is assigned to the π−π* ligand-centered (LC) transition, and the second one at lower energy (280−320 nm, (12−28) × 10^3 L·mol^{-1}·cm^{-1}) is ascribed to the dπ−π* metal-to-ligand charge transfer (MLCT) absorption.

Emission spectra, recorded in the solid state, display a very weak emission around 650 nm for the complexes **1**, **3**, **4**, and **10** and a broad emission around 436−488 nm for the dipyridylamine coordinated complexes **5**−**8** and **11**. To our knowledge, this is the first example of blue emitting mononuclear cationic NHC Cu(I) complexes.[12] The lack of luminescence of complexes **1**, **3**, **4**, and **10** cannot be attributed to a π−π stacking of the dinitrogenated based ligand as no emission was observed in the solid state for [Cu(IPr)(4,4′-di-*tert*-butyl-2,2′-bypyridine)][PF_6] copper complex (**22**) (Supporting Information, Figures S8 and S9). Noteworthy, almost no emission was observed in solution ($CHCl_3$) which is in good agreement with the work of Thompson.[12b] Copper complexes in solution are known to form excimers, decreasing the luminescence intensity. Nevertheless, when copper complexes bearing **L5**−**L8** as N^N ligand were irradiated under UV light (366 nm), a strong blue luminescence was observed in the solid state. Exploring this preliminary observation, the φ_{em} were measured between 5 to 88% with τ_{em} 17 to 78 μs (Table 4).

In this library of copper complexes, both [Cu(IPr)(**L6**)]-[PF_6] (**6**) and [Cu(SIPr)(**L5**)][PF_6] (**11**) show the highest φ_{em} with 86% (τ_{em} = 78 μs) and 88% (τ_{em} = 51 μs), respectively. The presence and position of the methyl groups on Hdpa appeared to play a crucial role on the φ_{em}. Indeed, the quantum yield of [Cu(IPr)(**L6**)][PF_6] (**6**) is four times as important as of [Cu(IPr)(**L5**)][PF_6] (**5**), whereas the quantum yield of [Cu(IPr)(**L7**)][PF_6] (**7**) is four times less than that of [Cu(IPr)(**L5**)][PF_6] (**5**). Then, saturated and unsaturated NHC ligand revealed also a strong impact on the φ_{em} as this value was found four times higher with [Cu(SIPr)(**L5**)][PF_6] (**11**) than with [Cu(IPr)(**L5**)][PF_6] (**5**).

Electrochemical Study. As one of the key point for OLED application is the reversibility of redox processes,[4] voltammetric experiments were carried out on copper complexes bearing planar (**L1**, **L3**, and **L4**) and nonplanar N^N ligands (**L5**−**L8**). Redox potentials are summarized in Table 5.

Complexes bearing **L1**, **L3**, or **L4** ligands (Figure 5) exhibit an irreversible reduction at around −1.8 V_{SCE}, which was assigned to a single ligand reduction and formation of [Cu(NHC)($L^{\bullet-}$)][0,25] and an irreversible CuI/CuII oxidation at 1.5 V_{SCE} which might be also due to a single ligand oxidation. Copper complexes coordinated to **L5**−**L8** ligands undergo an irreversible Cu^I/Cu^0 reduction at around −1.9 V_{SCE}. Because of

dx.doi.org/10.1021/ic501230m | Inorg. Chem. 2014, 53, 9181−9191

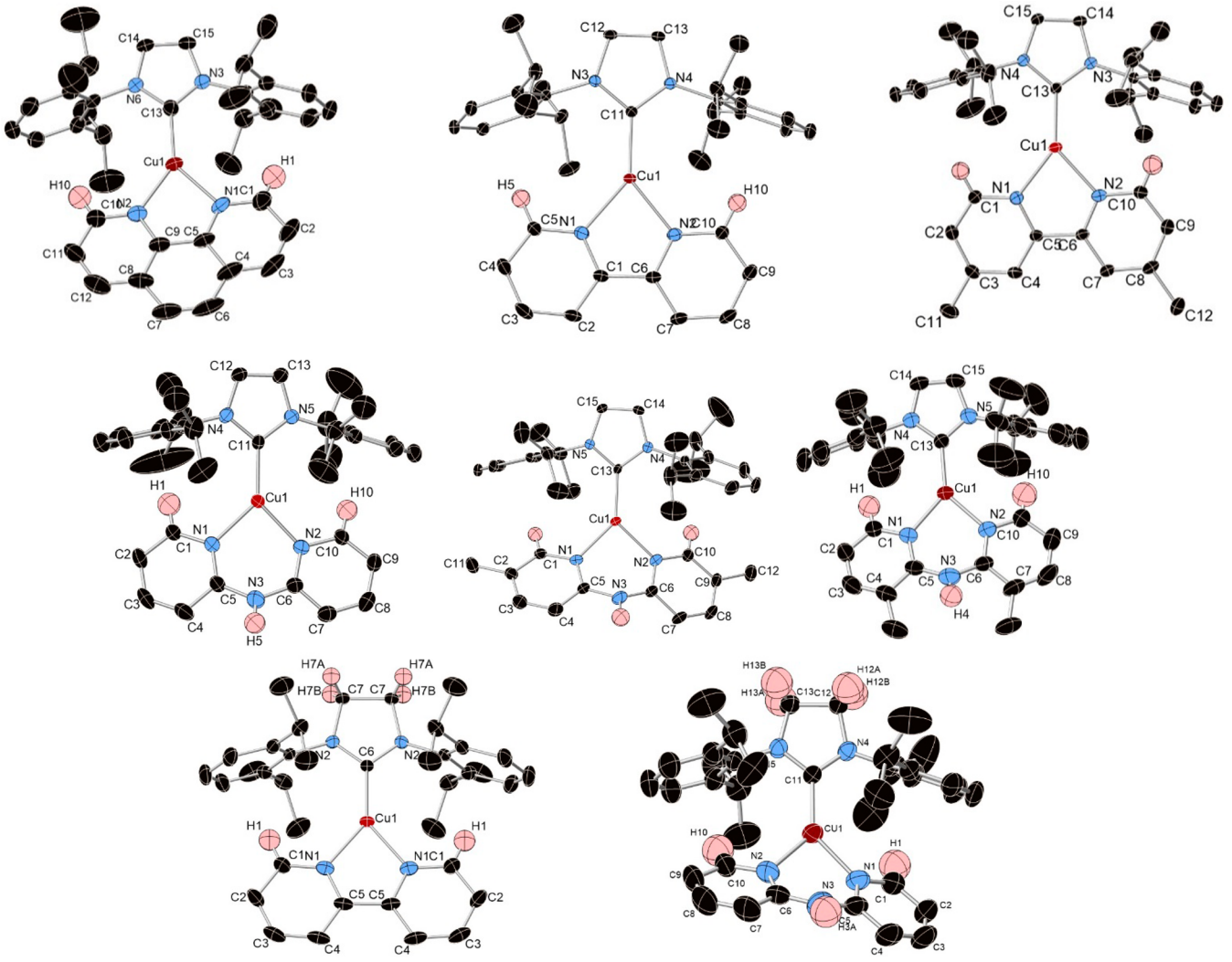

Figure 3. Thermal ellipsoid representations (50% probability) of [Cu(IPr)(**L1**)][BF_4] (**19**), [Cu(IPr)(**L3**)][BF_4] (**20**), [Cu(IPr)(**L4**)][PF_6] (**4**), [Cu(IPr)(**L5**)][PF_6] (**5**), [Cu(IPr)(**L6**)][PF_6] (**6**), [Cu(IPr)(**L8**)][PF_6] (**8**), [Cu(SIPr)(**L3**)][PF_6] (**10**), and [Cu(SIPr)(**L5**)][PF_6] (**11**) complexes. Some hydrogen atoms and counteranion were omitted for clarity.

the presence of a NH function in the N^N ligand, an irreversible oxidation of the nitrogen atom was observed around 1.25 V_{SCE}. Such oxidation corresponds to previously described results with ruthenium Hdpa complexes.[26] This has been confirmed with the voltammetry of ligand **L5** showing an irreversible oxidation around 1.8 V_{SCE}. We assume that this irreversible oxidation might be due to water traces in our solution. Finally, these complexes having the oxidized central nitrogen atom presented a second irreversible oxidation around 2.0 V_{SCE}.

Computational Study. The following complexes were studied: [Cu(IPr)(**L1**)]$^+$, [Cu(IPr)(**L2**)]$^+$, [Cu(IPr)(**L3**)]$^+$, [Cu(IPr)(**L4**)]$^+$, [Cu(IPr)(**L5**)]$^+$, [Cu(IPr)(**L6**)]$^+$, [Cu(IPr)-(**L7**)]$^+$, [Cu(IPr)(**L8**)]$^+$, [Cu(IPr)(**L9**)]$^+$, [Cu(SIPr)(**L3**)]$^+$, [Cu(SIPr)(**L5**)]$^+$.

Geometry. Because of the C_{2v} symmetry of the ligands **L1**, **L3**, and **L4** and of the IPr and SIPr carbenes, the complexes formed with these two ligands adopt a C_{2v} symmetry. With such geometry, the hydrogen of the pyridine ring (α of the nitrogen) point at the center of the phenyl ring of the NHC forming a CH−π interaction (Figure 6). This weak interaction is also called antihydrogen bond because of the reduction of the C−H bond length, resulting in a blue shift in the IR.[27] A typical stabilization in the order of a kcal/mol is expected per interaction. Besides, complexes with **L5**−**L8** ligands have a C_s symmetry, due to the nonplanarity of the N^N ligands caused by the pyramidal nitrogen bridging the two pyridine frameworks. Then, the antihydrogen bond is weakening because of the loss of symmetry. The CH−π distances and the CH−π angles are smaller with ligands **L5**−**L8** than with ligands **L1**, **L3**, and **L4** (Figure 6 and Table 6). These specific interactions appeared to be crucial for the formation of the complex and permit to explain why the synthesis failed with the ICy NHC ancillary ligand (See Supporting Information, Table S6). Also, these calculations explain why ligands **L2** and **L9**, bearing a methyl in α position with respect to the nitrogen atom, were not suitable ligands. Geometry optimizations were also performed with the B3LYP[28] and M06[29] functionals. No significant difference was observed. (Results are presented in Supporting Information, Tables S7 and S8 and Figures S20 and S21.)

Electronic Structure. All complexes showed an important charge transfer. The highest occupied molecular orbital (HOMO) is mainly localized on the copper atom, while the

dx.doi.org/10.1021/ic501230m | Inorg. Chem. 2014, 53, 9181−9191

Table 3. Selected Bond Lengths and Angles of [Cu(NHC)(N^N)][X] Complexes

complex	Cu−$C_{carbene}$ (Å)	Cu···N_{ligand} (Å)	N_{ligand}···Cu···N_{ligand} (deg)	N_{ligand}···Cu···$C_{carbene}$ (deg)	CH···C_g (Å)
[Cu(IPr)(**L1**)][BF_4] (**19**)	1.893(5)	2.040(4)	81.27(17)	141.49(18)	2.60
				137.14(19)	2.57
		2.061(4)			
[Cu(IPr)(**L3**)][BF_4] (**20**)	1.8919(18)	2.0436(17)	80.04(7)	139.77(7)	2.61
				140.19(7)	2.82
		2.0557(16)			
[Cu(IPr)(**L4**)][PF_6] (**4**)	1.8825(19)	2.0187(18)	80.49(7)	141.82(8)	2.88
				136.98(8)	2.53
		2.0616(17)			
[Cu(IPr)(**L5**)][PF_6] (**5**)	1.918(4)	2.040(4)	90.12(19)	134.0(2)	2.56
				135.83(17)	2.42
		2.065(4)			
[Cu(IPr)(**L6**)][PF_6] (**6**)	1.9208(18)	2.0577(18)	89.62(7)	135.94(7)	2.97
				134.42(7)	2.59
		2.0590(17)			
[Cu(IPr)(**L8**)][PF_6] (**8**)	1.902(2)	2.037(2)	91.04(9)	136.06(1)	2.75
				131.84(9)	2.83
		2.040(2)			
[Cu(SIPr)(**L3**)][PF_6] (**10**)	1.891(2)	2.0469(15)	79.70(9)	140.15(5)	2.55
[Cu(SIPr)(**L5**)][PF_6] (**11**)	1.9072(17)	2.0442(18)	88.94(8)	132.79(7)	2.48
			2.0503(17)	137.79(7)	2.43

Table 4. Photophysical Properties of Copper Complexes

	absorption[a]	emission[b]				
complex	λ_{max} [nm] (ε [10^4 L·mol^{-1}·cm^{-1}])	λ_{em} [nm]	φ_{em} ± 0.05	τ_{em} [μs]	k_r [10^4 s^{-1}]	k_{nr} [10^4 s^{-1}]
[Cu(IPr)(**L1**)][PF_6] (**1**)	240 (2.60), 279 (2.82)		≥0.01			
[Cu(IPr)(**L3**)][PF_6] (**3**)	250 (1.64), 310 (1.54)		≥0.01			
[Cu(IPr)(**L4**)][PF_6] (**4**)	262 (1.62), 307 (1.55)		≥0.01			
[Cu(IPr)(**L5**)][PF_6] (**5**)	260 (2.31), 315 (1.37)	488	0.22	29	0.8	2.7
[Cu(IPr)(**L6**)][PF_6] (**6**)	259 (2.19), 310 (1.44)	436	0.86	78	1.1	0.2
[Cu(IPr)(**L7**)][PF_6] (**7**)	261 (2.32), 316 (1.26)	455	0.05	17	0.3	5.6
[Cu(IPr)(**L8**)][PF_6] (**8**)	256 (2.58), 316 (1.28)	460	0.43	44	1.0	1.4
[Cu(SIPr)(**L3**)][PF_6] (**10**)	257 (1.82), 308 (1.17)		≥0.01			
[Cu(SIPr)(**L5**)][PF_6] (**11**)	261 (3.10), 320 (1.25)	484	0.88	51	1.7	0.2

[a]In $CHCl_3$, concentration 10^{-4} mol L^{-1}. [b]In the solid state.

lowest unoccupied molecular orbital (LUMO) is mainly localized on the ligand (see the HOMO and LUMO for [Cu(IPr)(**L1**)]$^+$ and [Cu(IPr)(**L5**)]$^+$, Figure 7). Energy levels for the HOMO and LUMO for the different complexes are illustrated in Supporting Information, Figure S22 (see Table 7 for values). The HOMO level does not change significantly for all complexes even when saturated, and consequently more electron donor, SIPr carbene was used. On the other hand, the LUMO level is quite sensitive to the ligand nature, and two families appeared (Table 7, see Supporting Information, Figure S22). Complexes with ligands **L5**−**L8** exhibited a larger gap (~8.4 eV) than those with ligands **L1**, **L3**, and **L4** (~7.6 eV).

Excited States. Time-dependent density functional theory (TD-DFT) calculations were carried out on all complexes of photophysical interest to rationalize absorption and emission processes.[30] The presence of a copper center allows singlet−triplet intersystem crossing. Thereby, both first singlet−singlet and singlet−triplet transitions were considered. Two types of photochemical behaviors were observed depending on the ligand in the complexes.

On one hand, complexes involving **L1**, **L3**, and **L4** ligands exhibit $S_0 \rightarrow S_1$ and $S_0 \rightarrow T_1$ transitions, which are almost spatially identical, that is, metal−ligand charge transfer (MLCT) confirming the experimentally suggested d → π^* transition. It must be stressed that H → L transition is always the main MO contribution to both $S_0 \rightarrow S_1$ and $S_0 \rightarrow T_1$ transitions (see Supporting Information, Tables S9 and S10). On the other hand, complexes involving **L5**−**L8** exhibit different spatial $S_0 \rightarrow S_1$ and $S_0 \rightarrow T_1$ transitions. The former transition is systematically assigned to symmetric MLCT while the latter is assigned to a complex mixture of MLCT and ligand-centered CT (LC-CT) (see Supporting Information, Tables S9 and S10).

Joint experiments and theoretical calculations provide some general trends. Experimentally, no emission is observed for **L1**-, **L3**-, and **L4**-based complexes in contrast to **L5**−**L8**-based complexes (Table 4). It must be stressed that the long emission lifetimes (from 17 to 78 μs) suggest $T_1 \rightarrow S_0$ transitions.

Theoretical calculations are in good agreement with experiments: (i) **L1**, **L3**, and **L4** $T_1 \rightarrow S_0$ is a π^*−d transition, which is not radiative; (ii) **L5**−**L8** $T_1 \rightarrow S_0$ transition is a π^*−π transition, explaining the existence of photoluminescence for bis(2-pyridyl)amine-based complexes. Vertical excitation energies were calculated with the ωB97XD functional and are presented in Table 8.

dx.doi.org/10.1021/ic501230m | Inorg. Chem. 2014, 53, 9181−9191

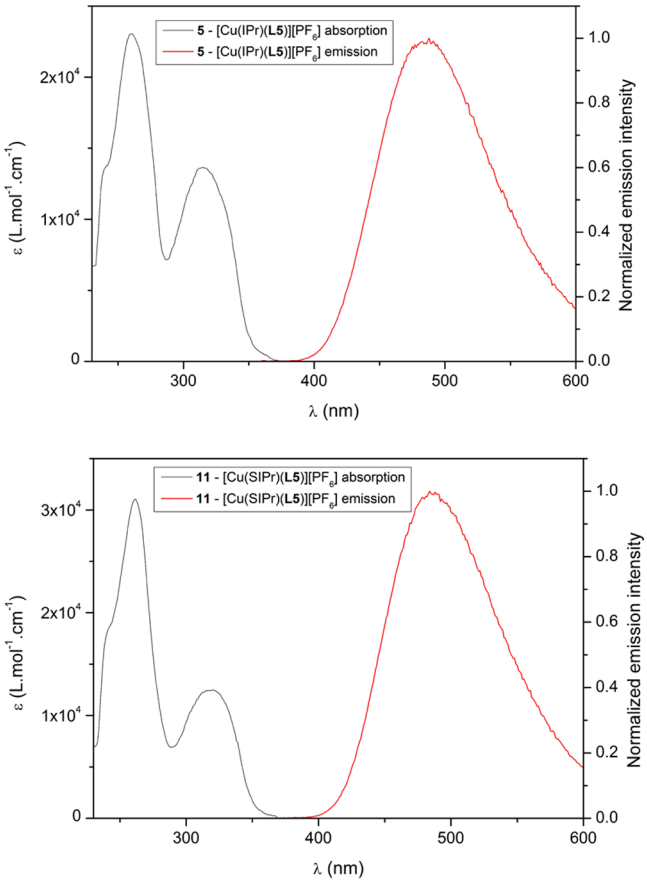

Figure 4. Absorption spectra of complexes **5** (top) and **11** (bottom) in $CHCl_3$ and emission spectra of complexes **5** (top) and **11** (bottom) in the solid state.

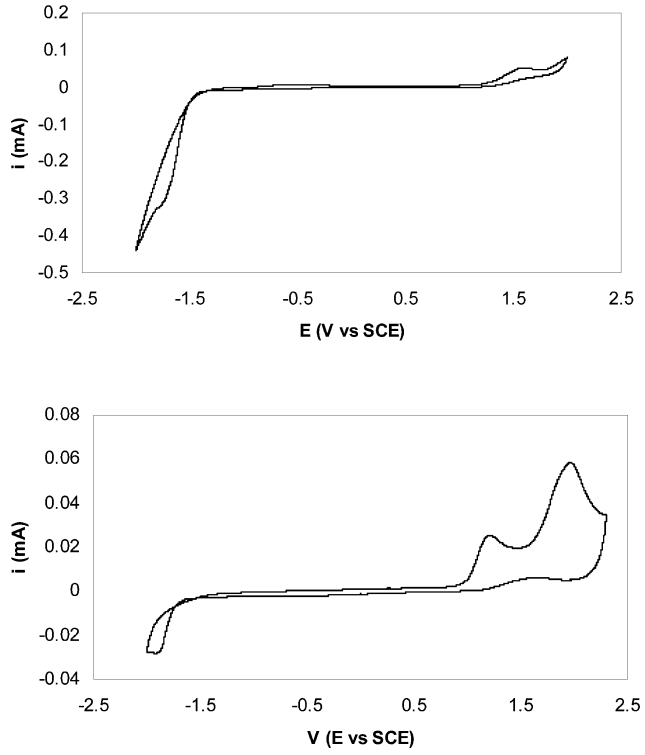

Figure 5. Cyclic voltammograms of complexes **1** (top) and **5** (bottom) in dichloromethane containing 0.1 M NBu_4PF_6. Scan rate = 0.025 $V{\cdot}s^{-1}$.

Excited-state geometries of nitrogen-based ligands are likely to play a crucial role to differentiate emission behaviors between both N^N ligands (i.e., **L1**, **L3**, and **L4** vs **L5**−**L8**). **L1**-, **L3**-, and **L4**-based complexes do not exhibit any degree of freedom that could allow geometry modification along excitation processes. On the other hand, **L5**−**L8**-based complexes present a central nitrogen atom that may planarize in the excited state and may undergo a modification of N atom hybridization from sp^3 to sp^2 along excitation. This might explain the existence of a stable triplet excited state contrary to **L1**-, **L3**-, and **L4**-based-complexes. A stable triplet state is necessary for emission processes. Therefore, the change of ligand geometry in our three-coordinated copper complexes is required to ensure the brightly blue emission. It is worth noting that such N-planarization must be distinguished from the flattening of four-coordinated copper complexes.[3b,8]

CONCLUSIONS

In conclusion, a new series of [Cu(NHC)(N^N)][X] complexes has been synthesized following two different procedures, starting either from [CuCl(NHC)] or [CuOH-(NHC)]. Interestingly, the surprising stability of these copper complexes results from CH−π system interactions between the hydrogen atoms at the α position of the nitrogen atoms in the N^N ligand and the aromatic ring of the NHC ligand. This explanation was also supported by DFT calculations. Furthermore, these complexes, bearing Hdpa derivatives as N^N ligands, presented very interesting photophysical properties. Indeed, these dipyridylamine ligands modify the geometry of the complex changing the common C_{2v} symmetry for complexes bearing planar N^N ligand to a C_s group. This structural modification leads to an increase of the HOMO−LUMO gap and results in a blue shift in the emission spectrum

Table 5. Redox Potential of Copper Complexes

complex	Ep_c (V_{SCE})	Ep_a (V_{SCE})	ΔE (V_{SCE})	Ep_a NH (V_{SCE})
[Cu(IPr)(**L1**)][PF_6] (**1**)	−1.78	1.60	3.38	
[Cu(IPr)(**L3**)][PF_6] (**3**)	−1.81	1.46	3.27	
[Cu(IPr)(**L4**)][PF_6] (**4**)	−1.87	1.43	3.30	
[Cu(IPr)(**L5**)][PF_6] (**5**)	−1.94	1.98		1.23
[Cu(IPr)(**L6**)][PF_6] (**6**)	−1.84	1.99		1.26
[Cu(IPr)(**L7**)][PF_6] (**7**)	−1.89	2.05		1.19
[Cu(IPr)(**L8**)][PF_6] (**8**)	−1.95	2.00		1.23
[Cu(SIPr)(**L3**)][PF_6] (**10**)	−1.77	1.39	3.16	
[Cu(SIPr)(**L5**)][PF_6] (**11**)	−2.25	2.12		1.27

dx.doi.org/10.1021/ic501230m | Inorg. Chem. 2014, 53, 9181−9191

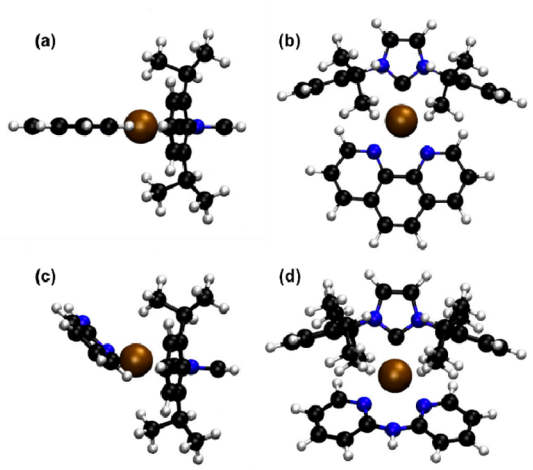

Figure 6. ωB97XD optimized structure of [Cu(IPr)(**L1**)]$^+$ side view (a) and top view (b) and [Cu(IPr)(**L5**)]$^+$ side view (c) and top view (d).

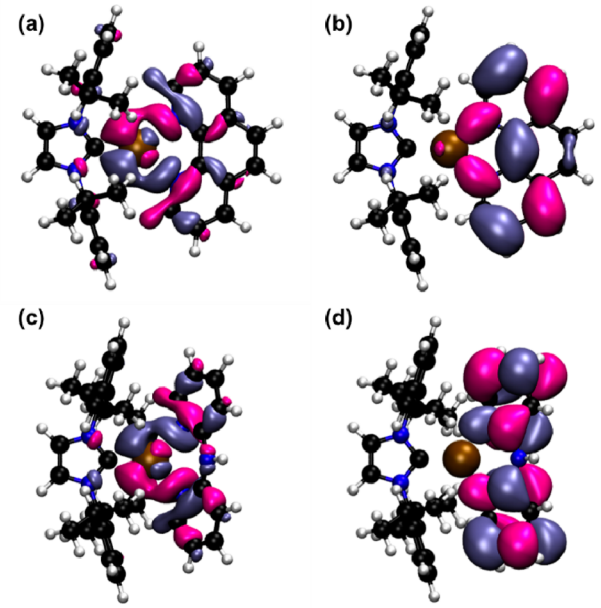

Figure 7. [Cu(IPr)(**L1**)]$^+$ HOMO (a) and LUMO (b) and [Cu(IPr)(**L5**)]$^+$ HOMO (c) and LUMO (d) obtained at the ωB97XD level.

in the solid state. All these results were supported and confirmed by DFT calculations. Finally, we are pleased to report here the first [Cu(NHC)(N^N)][X] complexes having high quantum yields in the blue region. These very thermally air-stable blue-emitting copper complexes present also a potential anchoring point with the bridged nitrogen atom of the dipyridylamine which can make them good candidates for OLED applications.

EXPERIMENTAL SECTION

Solvents were purchased from Carlo Erba and degassed prior to use by bubbling argon gas directly in the solvent. NMR spectra were recorded on a 400 and 500 MHz Bruker spectrometers. Proton (^{1}H) NMR information is given in the following format: multiplicity (s, singlet; d, doublet; t, triplet; q, quartet; qui, quintet; sept, septet; m, multiplet), coupling constant(s) (J) in Hertz (Hz), number of protons. The prefix *app* is occasionally applied when the true signal multiplicity was unresolved and br indicates the signal in question broadened. Carbon (^{13}C) NMR spectra are reported in ppm (δ) relative to residual $CDCl_3$ (δ 77.0) unless otherwise noted. HRMS analyses were performed by LCMT analytical services. NMR solvent was passed through a pad of basic alumina before use. UV−visible absorption spectra were measured at room temperature in chloroform on a Jenway 6715 UV/vis spectrometer, wavelengths are given in nm and extinction coefficients ε are presented in L·mol^{-1}·cm^{-1}. Steady-state emission spectra and emission lifetime were recorded with solid state on an Horiba Jobin Yvon Fluoromax-4P spectrofluorometer. For measuring absolute solid-state emission quantum yield, an Horiba Jobin Yvon integrating sphere F-3018 was equipped to the Fluoromax-4P spectrofluorometer.

General Procedures for the Synthesis of [Cu(NHC)(N^N)][X] Complexes. (Method A) In a flame-dried Schlenk tube under argon atmosphere, [CuCl(NHC)] complex (1 equiv) and N^N ligand (1.05 equiv) were dissolved in degassed absolute ethanol and heated to reflux for 1 h. After cooling to room temperature (RT), a saturated aqueous solution of KPF_6 was added affording a white precipitate. The solid was washed with water and diethyl ether and then dried under vacuum. (Method B) In a flame-dried Schlenk tube under argon atmosphere, [Cu(OH)(NHC)] complex (1 equiv), N^N ligand (1 equiv), and $HBF_4{\cdot}OEt_2$ (1 equiv) were introduced in degassed and dry toluene (C = 0.1 M) and stirred at RT for 2 h. Pentane was added affording a precipitate. The solid was washed with pentane and dried under vacuum.

[Cu(IPr)(L1)][PF$_6$] (1). Following method A, the product was obtained as a pale brown solid with 56% yield. Following method B, the product was obtained as a pale brown solid with 78% yield. ^{1}H NMR ($CDCl_3$, 400 MHz): 1.07 (d, J = 6.8 Hz, 12H), 1.30 (d, J = 6.8 Hz, 12H), 2.69 (sept, J = 6.8 Hz, 4H), 6.74 (d, J = 3.6 Hz, 2H), 7.40 (s, 2H), 7.52 (d, J = 7.7 Hz, 4H), 7.59 (dd, J = 7.6 Hz et J = 4.8 Hz, 2H), 7.79 (t, J = 7.7 Hz, 2H), 7.91 (s, 2H), 8.45 (d, J = 8.0 Hz, 2H) ppm. ^{13}C NMR ($CDCl_3$, 100 MHz): 23.6 (q×4), 25.1 (q×4), 28.9 (d×4), 123.6 (d×2), 124.8 (d×4), 125.3 (d×2), 127.0 (d×2), 128.9 (s×2), 130.7 (d×2), 135.9 (s×2), 138.9 (d×2), 143.5 (s×2), 146.4

Table 6. Bond Distances and Angles for the Different Complexes Calculated with the ωB97XD Functional

complexes	Cu···C$_{carbene}$ (Å)	Cu···N (Å)	N···Cu···N (deg)	N···Cu···C (deg)	CH···Π^a (Å)	CH···Π^b (deg)
[Cu(IPr)(**L1**)]$^+$	1.894	2.082	80.380	139.380	2.485	168.982
[Cu(IPr)(**L3**)]$^+$	1.895	2.076	79.091	140.455	2.433	173.947
[Cu(IPr)(**L4**)]$^+$	1.893	2.072	79.102	140.449	2.442	173.229
[Cu(IPr)(**L5**)]$^+$	1.912	2.077	89.261	134.760	2.554	125.8992
[Cu(IPr)(**L6**)]$^+$	1.912	2.075	89.255	134.739	2.565	124.624
[Cu(IPr)(**L7**)]$^+$	1.916	2.075	89.300	134.922	2.522	127.818
[Cu(IPr)(**L8**)]$^+$	1.912	2.075	89.750	134.719	2.664	123.013
[Cu(SIPr)(**L3**)]$^+$	1.905	2.081	78.903	140.549	2.397	174.351
[Cu(SIPr)(**L5**)]$^+$	1.921	2.082	88.885	134.815	2.542	125.147

^{a}Distance between the hydrogen and the phenyl ring center. ^{b}Angle between the carbon−hydrogen−phenyl ring center.

dx.doi.org/10.1021/ic501230m | Inorg. Chem. 2014, 53, 9181−9191

Table 7. HOMO, LUMO Levels and HOMO-LUMO Levels & Gaps for the Different Complexes Calculated with wB97XD

entry	HOMO (eV)	LUMO (eV)	HOMO−LUMO gap (eV)
[Cu(IPr)(**L1**)]$^+$	−10.68	−3.09	7.59
[Cu(IPr)(**L3**)]$^+$	−10.68	−3.12	7.56
[Cu(IPr)(**L4**)]$^+$	−10.52	−2.94	7.58
[Cu(IPr)(**L5**)]$^+$	−10.60	−2.19	8.41
[Cu(IPr)(**L6**)]$^+$	−10.45	−2.07	8.39
[Cu(IPr)(**L7**)]$^+$	−10.45	−2.00	8.45
[Cu(IPr)(**L8**)]$^+$	−10.44	−2.03	8.41
[Cu(SIPr)(**L3**)]$^+$	−10.69	−3.11	7.58
[Cu(SIPr)(**L5**)]$^+$	−10.62	−2.17	8.45

Table 8. Vertical Transition Energies, Absorption Wavelength, Main MO Description for Both First Singlet−Singlet ($S_0 \rightarrow S_1$) and Singlet−Triplet ($S_0 \rightarrow T_1$) Transitions

	S0→ S1			S0→T1		
complex	E [eV]	λ [nm]	main MO contribution	E [eV]	λ [nm]	main MO contribution
[Cu(IPr)(**L1**)]$^+$	3.4	363.4	H→L (68%)	3.2	381.6	H→L (67%)
[Cu(IPr)(**L3**)]$^+$	3.3	373.9	H→L (68%)	3.2	393.3	H→L (67%)
[Cu(IPr)(**L4**)]$^+$	3.4	367.4	H→L (68%)	3.2	388.3	H-5→L (54%)
[Cu(IPr)(**L5**)]$^+$	4.1	303.9	H→L+1 (58%)	3.5	350.2	H-1→L (48%)
[Cu(IPr)(**L6**)]$^+$	4.1	305.1	H-1→L +1(57%)	3.5	356.1	H→L (52%)
[Cu(IPr)(**L7**)]$^+$	3.9	314.3	H→L +1(54%)	3.6	348.2	H-1→L (50%)
[Cu(IPr)(**L8**)]$^+$	3.9	319.1	H-1→L+1 (57%)	3.5	350.7	H→L (53%)
[Cu(SIPr)(**L3**)]$^+$	3.3	372.7	H→L (68%)	3.2	391.6	H→L (67%)
[Cu(SIPr)(**L5**)]$^+$	3.8	325.9	H→L+1 (54%)	3.5	349.3	H-1→L (48%)

(s×4), 149.7 (d×2), 183.0 (s) ppm. HRMS (ESI): m/z calcd for $C_{39}H_{44}CuN_4$ [M−PF_6]$^+$: 631.2862; found: 631.2842. IR (neat): ν 3160, 3137, 2962, 1594, 1514, 1472, 1329, 1061, 837 cm^{-1}.

[Cu(IPr)(L3)][PF$_6$] (**3**). Following method A, the product was obtained as a pale brown solid with 72% yield. ^{1}H NMR ($CDCl_3$, 400 MHz): 1.07 (d, J = 6.8 Hz, 12H), 1.28 (d, J = 6.8 Hz, 12H), 2.64 (sept, J = 6.8 Hz, 4H), 6.31 (d, J = 4.6 Hz, 2H), 7.17 (t, J = 5.4 Hz, 2H), 7.33 (s, 2H), 7.47 (d, J = 7.8 Hz, 4H), 7.72 (t, J = 7.7 Hz, 2H), 7.98 (t, J = 6.8 Hz, 2H), 8.21 (d, J = 8.0 Hz, 2H) ppm. ^{13}C NMR ($(CD_3)_2CO$, 100 MHz): 22.9 (q×4), 24.2 (q×4), 28.7 (d×4), 121.9 (d×2), 124.3 (d×2), 124.7 (d×4), 126.2 (d×2), 130.6 (d×2), 136.3 (s×2), 140.3 (d×2), 146.3 (s×4), 149.6 (d×2), 152.0 (s×2), 182.4 (s) ppm. HRMS (ESI): m/z calcd for $C_{37}H_{44}CuN_4$ [M−PF_6]$^+$: 607.2862; found: 607.2869. IR (neat): ν 3162, 3135, 2966, 1595, 1471, 1329, 1060, 838 cm^{-1}.

[Cu(IPr)(L4)][PF$_6$] (**4**). Following method A, the product was obtained as a pale yellow solid with 94% yield. ^{1}H NMR ($CDCl_3$, 400 MHz): 1.07 (d, J = 6.8 Hz, 12H), 1.27 (d, J = 6.8 Hz, 12H), 2.44 (s, 6H), 2.63 (sept, J = 6.8 Hz, 4H), 6.15 (d, J = 5.3 Hz, 2H), 6.94 (d, J = 5.2 Hz, 2H), 7.31 (s, 2H), 7.45 (d, J = 7.8 Hz, 4H), 7.70 (t, J = 7.8 Hz, 2H), 8.04 (s, 2H) ppm. ^{13}C NMR ($CDCl_3$, 100 MHz): 21.2 (q×2), 23.6 (q×4), 24.9 (q×4), 28.8 (d×4), 122.5 (d×2), 123.4 (d×2), 124.6 (d×4), 126.5 (d×2), 130.5 (d×2), 135.9 (s×2), 146.3 (s×4), 148.8 (d×2), 151.9 (s×2), 152.2 (s×2), 183.2 (s) ppm. HRMS (ESI): m/z calcd for $C_{39}H_{48}CuN_4$ [M−PF_6]$^+$: 635.3175; found: 635.3179. IR (neat): ν 3174, 3130, 2965, 1613, 1557, 1470, 1408, 1329, 1059, 837 cm^{-1}.

[Cu(IPr)(L5)][PF$_6$] (**5**). Following method A, the product was obtained as a white solid with 72% yield. ^{1}H NMR ($CDCl_3$, 400 MHz): 1.08 (d, J = 6.9 Hz, 12H), 1.23 (d, J = 6.9 Hz, 12H), 2.65 (sept, J = 6.9 Hz, 4H), 6.17 (d, J = 5.4 Hz, 2H), 6.31 (t, J = 6.4 Hz, 2H), 7.16 (d, J = 8.5 Hz, 2H), 7.22 (s, 2H), 7.33 (d, J = 7.8 Hz, 4H), 7.48 (t, J = 7.5 Hz, 2H), 7.58 (t, J = 7.8 Hz, 2H), 8.08−8.13 (*br* s, NH) ppm. ^{13}C NMR ($CDCl_3$, 100 MHz): 23.9 (q×4), 24.2 (q×4), 28.7 (d×4), 115.0 (d×2), 116.4 (d×2), 123.5 (d×2), 124.7 (d×4), 130.6 (d×2), 135.9 (s×2), 139.1 (d×2), 146.0 (s×4), 147.5 (d×2), 152.9 (s×2), 183.0 (s) ppm. HRMS (ESI): m/z calcd for $C_{37}H_{45}CuN_5$ [M−PF_6]$^+$: 622.2971; found: 622.2981. IR (neat): ν 3385, 3170, 3133, 2963, 1629, 1582, 1471, 1229, 1160, 1061, 831 cm^{-1}.

[Cu(IPr)(L6)][PF$_6$] (**6**). Following method A, the product was obtained as a white solid with 98% yield. ^{1}H NMR ($CDCl_3$, 400 MHz): 1.07 (d, J = 6.6 Hz, 12H), 1.23 (d, J = 6.6 Hz, 12H), 2.33 (s, 6H), 2.65 (sept, J = 6.6 Hz, 4H), 6.20 (d, J = 4.2 Hz, 2H), 6.40 (t, J = 5.9 Hz, 2H), 6.71−6.76 (*br* s, NH), 7.22−7.28 (m and $CDCl_3$ signal overlapping, 2H), 7.33 (d, J = 7.6 Hz, 4H), 7.46 (d, J = 6.8 Hz, 2H), 7.59 (t, J = 7.7 Hz, 2H) ppm. ^{1}H NMR ($(CD_3)_2CO$, 400 MHz): 1.14 (d, J = 6.9 Hz, 12H), 1.25 (d, J = 6.9 Hz, 12H), 2.45 (s, 6H), 2.80 (sept, J = 6.9 Hz, 4H), 6.39 (d, J = 5.2 Hz, 2H), 6.60 (t, J = 6.4 Hz, 2H), 7.22−7.27 (br s, NH), 7.46 (d, J = 7.8 Hz, 4H), 7.67 (t, J = 7.5 Hz, 4H), 7.80 (s, 2H) ppm. ^{13}C NMR ($CDCl_3$, 100 MHz): 17.1 (q×2), 24.0 (q×4), 24.2 (q×4), 28.7 (d×4), 117.3 (d×2), 121.4 (s×2), 123.6 (d×2), 124.7 (d×4), 130.7 (d×2), 135.9 (s×2), 140.2 (d×2), 146.0 (s×4), 146.0 (d×2), 150.8 (s×2), 182.6 (s) ppm. HRMS (ESI): m/z calcd for $C_{39}H_{49}CuN_5$ [M−PF_6]$^+$: 650.3284; found: 650.3265. IR (neat): ν 3455, 3172, 3135, 2967, 1620, 1592, 1521, 1462, 1118, 1061, 836 cm^{-1}.

[Cu(IPr)(L7)][PF$_6$] (**7**). Following method A, the product was obtained as a white solid with 93% yield. ^{1}H NMR ($CDCl_3$, 400 MHz): 1.08 (d, J = 6.8 Hz, 12H), 1.23 (d, J = 6.8 Hz, 12H), 2.19 (s, 6H), 2.66 (sept, J = 6.8 Hz, 4H), 5.97 (d, J = 5.7 Hz, 2H), 6.11 (d, J = 5.6 Hz, 2H), 6.92 (s, 2H), 7.21 (s, 2H), 7.34 (d, J = 7.8 Hz, 4H), 7.58 (t, J = 7.7 Hz, 2H), 7.86−7.92 (br s, NH) ppm. ^{13}C NMR ($CDCl_3$, 100 MHz): 20.9 (q×2), 24.0 (q×4), 24.2 (q×4), 28.7 (d×4), 114.8 (d×2), 117.7 (d×2), 123.4 (d×2), 124.7 (d×4), 130.6 (d×2), 136.0 (s×2), 146.0 (s×4), 147.1 (d×2), 150.8 (s×2), 152.9 (s×2), 183.5 (s) ppm. HRMS (ESI): m/z calcd for $C_{39}H_{49}CuN_5$ [M−PF_6]$^+$: 650.3284; found: 650.3289. IR (neat): ν 3405, 3174, 3133, 2962, 1633, 1579, 1526, 1476, 1399, 1190, 838 cm^{-1}.

[Cu(IPr)(L8)][PF$_6$] (**8**). Following method A, the product was obtained as a white solid with 73% yield. ^{1}H NMR ($CDCl_3$, 400 MHz): 1.11 (d, J = 6.9 Hz, 12H), 1.22 (d, J = 6.9 Hz, 12H), 1.93 (s, 6H), 2.72 (sept, J = 6.9 Hz, 4H), 6.33 (s, 2H), 7.08 (d, J = 8.6 Hz, 2H), 7.19 (s, 2H), 7.30 (d, J = 7.7 Hz, 4H), 7.32 (d, J = 8.0 Hz, 2H), 7.52 (t, J = 7.7 Hz, 2H), 7.85−7.91 (br s, NH) ppm. ^{13}C NMR ($CDCl_3$, 100 MHz): 17.9 (q×2), 24.0 (q×4), 24.1 (q×4), 28.7 (d×4), 114.7 (d×2), 123.4 (d×2), 124.3 (d×4), 125.6 (s×2), 130.6 (d×2), 135.8 (s×2), 140.5 (d×2), 145.8 (s×4), 146.2 (d×2), 151.2 (s×2), 152.9 (s×2), 183.5 (s) ppm. HRMS (ESI): m/z calcd for $C_{39}H_{49}CuN_5$

dx.doi.org/10.1021/ic501230m | *Inorg. Chem.* 2014, 53, 9181−9191

$[M-PF_6]^+$: 650.3284; found: 650.3286. IR (neat): ν 3390, 3174, 3132, 2963, 1625, 1580, 1482, 1377, 1232, 1044, 828 cm^{-1}.

*[Cu(SIPr)(L3)][PF$_6$] (**10**).* Following method A, the product was obtained as a pale brown solid with 88% yield. ^{1}H NMR ($CDCl_3$, 400 MHz): 1.11 (d, J = 6.9 Hz, 12H), 1.39 (d, J = 6.9 Hz, 12H), 3.16 (sept, J = 6.9 Hz, 4H), 4.18 (s, 4H), 6.13 (d, J = 5.0 Hz, 2H), 7.11 (t, J = 5.0 Hz, 2H), 7.41 (d, J = 7.8 Hz, 4H), 7.62 (t, J = 7.8 Hz, 2H), 7.94 (t, J = 6.4 Hz, 2H), 8.16 (d, J = 8.0 Hz, 2H) ppm. ^{13}C NMR ($(CD_3)_2CO$, 100 MHz): 23.0 (q×4), 25.0 (q×4), 28.6 (d×4), 53.7 (t×2), 121.8 (d×2), 125.1 (d×4), 126.1 (d×2), 129.8 (d×2), 136.6 (s×2), 140.3 (d×2), 147.6 (s×4), 149.8 (d×2), 151.9 (s×2), 204.8 (s) ppm. HRMS (ESI): m/z calcd for $C_{37}H_{46}CuN_4$ $[M-PF_6]^+$: 609.3018; found: 609.2997. IR (neat): ν 3162, 3134, 2965, 1599, 1442, 1270, 1059, 836 cm^{-1}.

*[Cu(SIPr)(L5)][PF$_6$] (**11**).* Following method A, the product was obtained as a white solid with 81% yield. ^{1}H NMR ($CDCl_3$, 400 MHz): 1.16 (d, J = 6.9 Hz, 12H), 1.34 (d, J = 6.9 Hz, 12H), 3.13 (sept, J = 6.9 Hz, 4H), 4.07 (s, 4H), 6.16 (d, J = 4.7 Hz, 2H), 6.29 (t, J = 5.9 Hz, 2H), 7.12 (d, J = 8.7 Hz, 2H), 7.23–7.29 (m and $CDCl_3$ signal overlapping, 4H), 7.46 (t, J = 7.6 Hz, 4H), 8.05–8.10 (br s, NH) ppm. ^{1}H NMR ($(CD_3)_2CO$, 400 MHz): 1.21 (d, J = 6.8 Hz, 12H), 1.33 (d, J = 6.8 Hz, 12H), 3.36 (sept, J = 6.8 Hz, 4H), 4.27 (s, 4H), 6.36 (d, J = 5.4 Hz, 2H), 6.55 (t, J = 6.5 Hz, 2H), 7.02 (d, J = 8.3 Hz, 2H), 7.39 (d, J = 7.7 Hz, 4H), 7.54 (t, J = 7.9 Hz, 2H), 7.68 (t, J = 7.3 Hz, 2H), 9.62–9.66 (br s, NH) ppm. ^{13}C NMR ($CDCl_3$, 100 MHz): 24.2 (q×4), 24.7 (q×4), 28.8 (d×4), 53.8 (t×2), 114.8 (d×2), 116.3 (d×2), 125.0 (d×4), 129.8 (d×2), 136.2 (s×2), 139.0 (d×2), 147.0 (s×4), 147.6 (d×2), 152.8 (s×2), 205.6 (s) ppm. HRMS (ESI): m/z calcd for $C_{37}H_{47}CuN_5$ $[M-PF_6]^+$: 624.3127; found: 624.3116. IR (neat): ν 3387, 3164, 3133, 2961, 1630, 1583, 1472, 1367, 1272, 1160, 1057, 829 cm^{-1}.

X-ray Crystallography. Crystallographic data sets were collected from single crystal samples. Collections were performed using a Bruker Kappa APEXII CCD diffractometer. The initial unit cell parameters were determined by a least-squares fit of the angular setting of strong reflections, collected by a 6.0° scan in 12 frames over three different parts of the reciprocal space (36 frames total). Cell refinement and data reduction were performed with SAINT (Bruker AXS). Absorption correction was done by multiscan methods using SADABS-2012/1 (Bruker AXS). The structure was solved by direct methods and refined using either SHELXL-97 or SHELXL-2013 (Sheldrick). All non-H atoms were refined by full-matrix least-squares with anisotropic displacement parameters while hydrogen atoms were placed in idealized positions. Crystal data and details of the data collection and refinement are summarized in Supporting Information, Tables S1–S3. CCDC numbers (988571–988578) contain the supplementary crystallographic data for this article. These data can be obtained free of charge from the Cambridge Crystallographic Data Centre via www.ccdc.cam.ac.uk/data_request/cif.

Computational Details. Calculations were performed with the Gaussian 09 package.[31] Ground states geometries were optimized using the ωB97XD functional,[32] which is a long-range corrected functional and has been parametrized to take into account dispersive forces. The effective core potential SDD was used for the copper atom and the 6-31+G(d,p) basis set for carbon, nitrogen and hydrogen. Frequency calculations were performed to ensure that the obtained geometries were in the global minimum of the potential energy surface. TD-DFT calculations were performed at the same level of theory. Inorganic complexes are expected to undergo excited state charge transfer (e.g., MLCT, LC-CT).[32,33] Classical hybrid functionals (e.g., B3LYP) are well-known to fail at describing such event. This can be overcome by using range-separated formalism as in ωB97XD. Over the past year, this has shown reliable results with excited state charge transfer in organic[34] and inorganic systems.[35]

The S0, S1, and T1 densities for each studied complexes (Supporting Information, Tables S9 and S10) were done via natural transition orbitals (NTO). This successful approach aims at plotting the global MO distributions for both GS and ES in which all MOs involved in the electronic transition of interest are weighted by the CI coefficients.[36] Visualization has been performed with the VMD program.[37]

■ ASSOCIATED CONTENT

Ⓢ Supporting Information

X-ray crystallographic data for complexes **4**, **5**, **6**, **8**, **10**, **11**, **19**, and **20** in CIF format. Additional synthesis procedure for complexes **1**–**18**, **22**, and ligands **L6**–**L9**; crystallographic and structure refinement data; absorption and emission spectra of other copper complexes, cyclic voltamogramm of other copper complexes, additional DFT studies. This material is available free of charge via the Internet at http://pubs.acs.org.

■ AUTHOR INFORMATION

Corresponding Authors

*E-mail: mathieu@ifm.liu.se. (M.L.)
*E-mail: matthieu.hamel@cea.fr. (M.H.)
*E-mail: sylvain.gaillard@ensicaen.fr. (S.G.)

Author Contributions

The manuscript was written through contributions of all authors. All authors have given approval to the final version of the manuscript.

Notes

The authors declare no competing financial interest.

■ ACKNOWLEDGMENTS

This work was supported by the Ministère de la Recherche et des Nouvelles Technologies, Centre National de la Recherche Scientifique (CNRS). We thank the Agence Nationale de la Recherche, within the CSOSG program (ANR-12-SECU-0002-02), and the Région Basse-Normandie for their funding (R.M. and F.S.). The LABEX SynOrg (ANR-11-LABX-0029) is acknowledged for a Ph.D. grant (E.S.). M.L. acknowledges SeRC (Swedish e-Science Research Center) for funding as well as SNIC (Swedish National Infrastructure for Computing) for providing computer resources (snic001-12-192). The authors warmly thank Dr. F. Geneste for helpful scientific discussions.

■ REFERENCES

(1) (a) Keefe, M. H.; Benkstein, K. D.; Hupp, J. T. *Coord. Chem. Rev.* **2000**, *205*, 201–228. For recent reviews on iridium complexes, see: (b) You, Y.; Nam, W. *Chem. Soc. Rev.* **2012**, *41*, 7061–7084. (c) Li, S. P.-Y.; Zhang, K. Y. *New J. Chem.* **2011**, *35*, 265–287. (d) Liu, Z.; Bian, Z.; Huang, C. *Top. Organomet. Chem.* **2010**, *28*, 113–142. (e) Lowry, S. L.; Bernhard, S. *Chem.—Eur. J.* **2006**, *12*, 7970–7977. For recent reviews on platinum complexes, see: (f) Williams, J. A. G.; Develay, S.; Rochester, D. L.; Murphy, L. *Coord. Chem. Rev.* **2008**, *252*, 2596–2611. (g) Wong, K. M.-C.; Yam, V. W.-W. *Coord. Chem. Rev.* **2007**, *251*, 2477–2488.

(2) Yersin, H. *Highly Efficient OLEDs with Phosphorescent Materials;* Wiley-VCH Verlag GmbH & Co. KGaA: Weinheim, Germany, 2008.

(3) (a) Greenwood, N.; Earnshaw, A. *Chemistry of the Elements,* 2nd ed.; Elsevier: Oxford, U.K., 1997. (b) Wallesh, M.; Volz, D.; Zink, D. M.; Schepers, U.; Nieger, M.; Baumann, T.; Bräse, S. *Chem.—Eur. J.* **2014**, *20*, 6578–6590. (c) Zink, D. M.; Bächle, M.; Baumann, T.; Nieger, M.; Kühn, M.; Wang, C.; Klopper, W.; Monkowius, Hofbeck; Yersin, H.; Bräse, S. *Inorg. Chem.* **2013**, *52*, 2292–2305. (d) Volz, D.; Nieger, M.; Friedrichs, J.; Baumann, T.; Bräse, S. *Langmuir* **2013**, *29*, 3034–3044.

(4) Evans, R. C.; Douglas, P.; Winscom, C. J. *Coord. Chem. Rev.* **2006**, *250*, 2093–2126.

(5) Hasimoto, M.; Igawa, S.; Yashima, M.; Kawata, I.; Hoshino, M.; Osawa, M. J. *Am. Chem. Soc.* **2011**, *133*, 10348–10351.

(6) (a) Voltz, D.; Baumann, T.; Flügge, H.; Mydlak, M.; Grab, T.; Bächle, M.; Barner-Kowollik, C.; Bräse, S. *J. Mater. Chem.* **2012**, *22*,

20786−20790. (b) Liu, Z.; Qayyum, M. F.; Wu, C.; Whited, M. T.; Djurovich, P. I.; Hodgson, K. O.; Hedman, B.; Solomon, E. I.; Thompson, M. E. J. *Am. Chem. Soc.* **2011**, *133*, 3700−3703. (c) Deaton, J. C.; Switalski, S. C.; Kondakov, D. Y.; Young, R. H.; Pawlik, T. D.; Giesen, D. J.; Harkins, S. B.; Miller, A. J. M.; Mickenberg, S. F.; Peters, J. C. *J. Am. Chem. Soc.* **2010**, *132*, 9499−9508. (d) Tsuboyama, A.; Kuge, K.; Furugori, M.; Okada, S.; Hoshino, S.; Ueno, K. *Inorg. Chem.* **2007**, *46*, 1992−2001.

(7) (a) Igawa, S.; Hashimoto, M.; Kawata, I.; Yashima, M.; Hoshino, M.; Osawa, M. *J. Mater. Chem. C* **2013**, *1*, 542−551. (b) Hsu, C.-W.; Lin, C.-C.; Chung, M.-W.; Chi, Y.; Lee, G.-H.; Chou, P.-T.; Chang, C.-H.; Chen, P.-Y. *J. Am. Chem. Soc.* **2011**, *133*, 12085−12099.

(8) (a) McMillin, D. R.; McNett, K. M. *Chem. Rev.* **1998**, *98*, 1201−1219. (b) Cunningham, C. T.; Moore, J. J.; Cunningham, K. L. H.; Fanwick, P. E.; McMillin, D. R. *Inorg. Chem.* **2000**, *39*, 3638−3644.

(9) Kaeser, A.; Mohankumar, M.; Mohanraj, J.; Monti, F.; Holler, M.; Cid, J.-J.; Moudam, O.; Nierengarten, I.; Karmazin-Brelot, L.; Duhayon, C.; Delavaux-Nicot, B.; Armaroli, N.; Nierengarten, J.-F. *Inorg. Chem.* **2013**, *52*, 12140−12151.

(10) For selected recent examples, see: (a) Hattori, Y.; Nishikawa, M.; Kusamoto, T.; Kume, S.; Nishihara, H. *Inorg. Chem.* **2014**, *53*, 231−2840. (b) Bergmann, L.; Friedrichs, J.; Mydlak, M.; Baumann, T.; Nieger, M.; Bräse, S. *Chem. Commun.* **2013**, *49*, 6501−6503. (c) Schweinfurth, D.; Büttner, N.; Hohloch, S.; Deibel, N.; Klein, J.; Sarkar, B. *Organometallics* **2013**, *32*, 5834−5842. (d) Femoni, C.; Muzzioli, S.; Palazzi, A.; Stagni, S.; Zacchini, S.; Monti, F.; Accorsi, G.; Bolognesi, M.; Armaroli, N.; Massi, M.; Valenti, G.; Marcaccio, M. *Dalton Trans.* **2013**, *42*, 997−1010. (e) Czerwieniec, R.; Kowalski, K.; Yersin, H. *Dalton Trans.* **2013**, *42*, 9826−9830. (f) Andrés-Tomé, I.; Fyson, J.; Baiao Dias, F.; Monkman, A. P.; Lacobellis, G.; Coppo, P. *Dalton Trans.* **2012**, *41*, 8669−8674. (g) Wada, A.; Zhang, Q.; Yasuda, T.; Takasu, I.; Enomoto, S.; Adachi, C. *Chem. Commun.* **2012**, *48*, 5340−5342. (h) Nishikawa, M.; Nomoto, K.; Kume, S.; Inoue, K.; Sakai, M.; Fujii, M.; Nishihara, H. *J. Am. Chem. Soc.* **2010**, *132*, 9579−9581.

(11) (a) Nelson, D. J.; Nolan, S. P. *Chem. Soc. Rev.* **2013**, *42*, 6723−6753. (b) Díez-González, S.; Nolan, S. P. *Coord. Chem. Rev.* **2007**, *251*, 874−883. (c) Scoot, N. M.; Nolan, S. P. *Eur. J. Inorg. Chem.* **2005**, 1815−1828.

(12) For a recent review on NHC metal complexes having photoluminescence properties, see: (a) Visbal, R.; Gimeno, M. C. *Chem. Soc. Rev.* **2014**, *43*, 3551−3574. (b) Krylova, V. A.; Djurovich, P. I.; Whited, M. T.; Thompson, M. E. *Chem. Commun.* **2010**, *46*, 6696−6698. (c) Krylova, V. A.; Djurovich, P. I.; Aronson, J. W.; Haiges, R.; Whited, M. T.; Thompson, M. E. *Organometallics* **2012**, *31*, 7983−7993. (d) Guo, S.; Lim, M. H.; Huynh, H. V. *Organometallics* **2013**, *32*, 7225−7233. (e) Catalano, V. J.; Munro, L. B.; Strasser, C. E.; Samin, A. F. *Inorg. Chem.* **2011**, *50*, 8465−8476. (f) Matsumoto, K.; Matsumoto, N.; Ishii, A.; Tsukuda, T.; Hasegawa, M.; Tsubomura, T. *Dalton Trans.* **2009**, 6795−6801.

(13) Gaillard, S.; Elmkaddem, M. K.; Fischmeister, C.; Thomas, C. M.; Renaud, J.-L. *Tetrahedron Lett.* **2008**, *49*, 3471−3474.

(14) (a) Zheng, Z.; Elmkaddem, M. K.; Fischmeister, C.; Roisnel, T.; Thomas, C. M.; Carpentier, J.-F.; Renaud, J.-L. *New J. Chem.* **2008**, *32*, 2150−2158. (b) Romain, C.; Gaillard, S.; Elmkaddem, M. K.; Toupet, L.; Fischmeister, C.; Thomas, C. M.; Renaud, J.-L. *Organometallics* **2010**, *29*, 1992−1995. (c) Sauvageot, E.; Marion, R.; Sguerra, F.; Grimault, A.; Daniellou, R.; Hamel, M.; Gaillard, S.; Renaud, J.-L. *Org. Chem. Front.* **2014**, *1*, 639−644.

(15) (a) Meyers, A.; Weck, M. *Macromolecules* **2003**, *36*, 1766−1768. (b) Furuta, P. T.; Deng, L.; Garon, S.; Thompson, M. E.; Fréchet, J. M. J. *J. Am. Chem. Soc.* **2004**, *126*, 15388−15389. (c) Wang, X.-Y.; Kimyonok, A.; Weck, M. *Chem. Commun.* **2006**, 3933−3935.

(16) (a) Sinner, F.; Buchmeiser, M. R.; Tessadri, R.; Mupa, M.; Wurst, K.; Bonn, G. K. *J. Am. Chem. Soc.* **1998**, *120*, 2790−2797. (b) Kröll, R.; Eschbaumer, C.; Schuber, U. S.; Buchmeiser, M. R.; Wurst, K. *Macromol. Chem. Phys.* **2001**, *202*, 645−653.

(17) (a) Ni, J.; Wei, K.-J.; Min, Y.; Chen, Y.; Zhan, S.; Li, D.; Liu, Y. *Dalton Trans.* **2012**, *41*, 5280−5293. (b) Xie, Y.; Ding, Y.; Wang, C.; Hill, J. P.; Ariga, K.; Zhang, W.; Zhu, W. *Chem. Commun.* **2012**, *48*, 11513−11515. (c) Martić, S.; Wu, G.; Wang, S. *Inorg. Chem.* **2008**, *47*, 8315−8323.

(18) (a) Liu, Q.-D.; Jia, W.-L.; Wu, G.; Wang, S. *Organometallics* **2003**, *22*, 3781−3791. (b) Lee, J.; Liu, Q.-D.; Motala, M.; Dane, J.; Gao, J.; Kang, Y.; Wang, S. *Chem. Mater.* **2004**, *16*, 1869−1877. (c) Bai, D.-R.; Wang, S. *Organometallics* **2006**, *25*, 1517−1524. (d) Tan, R.; Wang, Z.-B.; Li, Y.; Kozera, D. J.; Lu, Z.-H.; Song, D. *Inorg. Chem.* **2012**, *51*, 7039−7049.

(19) (a) Citadelle, C. A.; Le Nouy, E.; Bisaro, F.; Slawin, A. M. Z.; Cazin, C. S. J. *Dalton Trans.* **2010**, *39*, 4489−4491. (b) Santoro, O.; Collado, A.; Slawin, A. M. Z.; Nolan, S. P.; Cazin, C. S. J. *Chem. Commun.* **2013**, *49*, 10483−10485.

(20) (a) Díez-González, S.; Stevens, E. D.; Scott, N. M.; Petersen, J. L.; Nolan, S. P. *Chem.—Eur. J.* **2008**, *14*, 158−168. (b) Lazreg, F.; Slawin, A. M. Z.; Cazin, C. S. J. *Organometallics* **2012**, *31*, 7969−7975.

(21) Ruthkosky, M.; Castellano, F. N.; Meyer, G. J. *Inorg. Chem.* **1996**, *35*, 6406−6412.

(22) Fortman, G. C.; Slawin, A. M. Z.; Nolan, S. P. *Organometallics* **2010**, *29*, 3966−3972.

(23) $CDCl_3$ was filtered prior to use through a pad of basic alumina to remove HCl traces.

(24) (a) Suezawa, H.; Yoshida, T.; Umezawa, Y.; Tsuboyama, S.; Nishio, M. *Eur. J. Inorg. Chem.* **2002**, 3148−3155. (b) Nishio, M.; Hirota, M.; Umezawa, Y. *The CH/π Interaction—Evidence, Nature, and Consequences;* Wiley-VCH: New York, 1998.

(25) Miller, M. T.; Gantzel, P. K.; Karpishin, T. B. *Inorg. Chem.* **1999**, *38*, 3414−3422.

(26) Morris, D. E.; Ohsawa, Y.; Segers, D. P.; DeArmond, M. K.; Hanck, K. W. *Inorg. Chem.* **1984**, *23*, 3010−3017.

(27) Joseph, J.; Jemmis, E. D. *J. Am. Chem. Soc.* **2007**, *129*, 4620−4632.

(28) (a) Becke, A. D. *J. Chem. Phys.* **1993**, *98*, 5648−5652. (b) Lee, C.; Yang, W.; Parr, R. G. *Phys. Rev. B* **1988**, *37*, 785−789. (c) Vosko, S. H.; Wilk, L.; Nusair, M. *Can. J. Phys.* **1980**, *58*, 1200−1211. (d) Stephens, P. J.; Devlin, F. J.; Chabalowski, C. F.; Frisch, M. J. *J. Phys. Chem.* **1994**, *98*, 11623−11627.

(29) Zhao, Y.; Truhlar, D. G. *Theor. Chem. Acc.* **2008**, *120*, 215−241.

(30) It must be stressed that most of calculated transitions exhibited very weak oscillator strengths since they are forbidden them by symmetry. However, the presence of counterions breaks the symmetry in the crystal as it can be seen from X-ray structures. Consequently, those transitions are allowed.

(31) Frisch, M. J.; Trucks, G. W.; Schlegel, H. B.; Scuseria, G. E.; Robb, M. A.; Cheeseman, J. R.; Scalmani, G.; Barone, V.; Mennucci, B.; Petersson, G. A.; Nakatsuji, H.; Caricato, M.; Li, X.; Hratchian, H. P.; Izmaylov, A. F.; Bloino, J.; Zheng, G.; Sonnenberg, J. L.; Hada, M.; Ehara, M.; Toyota, K.; Fukuda, R.; Hasegawa, J.; Ishida, M.; Nakajima, T.; Honda, Y.; Kitao, O.; Nakai, H.; Vreven, T.; Montgomery, J. A., Jr.; Peralta, J. E.; Ogliaro, F.; Bearpark, M.; Heyd, J. J.; Brothers, E.; Kudin, K. N.; Staroverov, V. N.; Kobayashi, R.; Normand, J.; Raghavachari, K.; Rendell, A.; Burant, J. C.; Iyengar, S. S.; Tomasi, J.; Cossi, M.; Rega, N.; Millam, N. J.; Klene, M.; Knox, J. E.; Cross, J. B.; Bakken, V.; Adamo, C.; Jaramillo, J.; Gomperts, R.; Stratmann, R. E.; Yazyev, O.; Austin, A. J.; Cammi, R.; Pomelli, C.; Ochterski, J. W.; Martin, R. L.; Morokuma, K.; Zakrzewski, V. G.; Voth, G. A.; Salvador, P.; Dannenberg, J. J.; Dapprich, S.; Daniels, A. D.; Farkas, Ö.; Foresman, J. B.; Ortiz, J. V.; Cioslowski, J.; Fox, D. J. *Gaussian 09, Revision D.01;* Gaussian, Inc.: Wallingford, CT, 2009.

(32) Chai, J. D.; Head-Gordon, M. *Phys. Chem. Chem. Phys.* **2008**, *10*, 6615−6620.

(33) Chai, J.-D.; Head-Gordon, M. *J. Chem. Phys.* **2008**, *128*, 084106.

(34) Di Meo, F.; Sancho Garcia, J. C.; Dangles, O.; Trouillas, P. *J. Chem. Theory Comput.* **2012**, *8*, 2034−2043.

(35) Minenkov, Y.; Singstad, Å.; Occhipinti, G.; Jensen, V. R. *Dalton Trans.* **2012**, *41*, 5526−5541.

(36) Rustioni, L.; Di Meo, F.; Guillaume, M.; Failla, O.; Trouillas, P. *Food Chem.* **2013**, *141*, 4349−4357.

(37) Humphrey, W.; Dalke, A.; Schulten, K. *J. Mol. Graphics* **1996**, *14*, 33−38.

dx.doi.org/10.1021/ic501230m | *Inorg. Chem.* 2014, 53, 9181−9191